THE LASER TEXTURING OF CEMENTED CARBIDE SURFACES

Davi Neves, davis@ieav.cta.br
Anselmo Eduardo Diniz, anselmo@fem.unicamp.br
Faculdade de Engenharia Mecânica – Universidade Estadual de Campinas – CP 6122 – Campinas – SP – 13083-970

Milton Sérgio Fernandes de Lima, msflima@yahoo.com.br
Divisão de Fotonica – Instituto de Estudos Avançados – IEAV/DCTA – CP 6044 – São José dos Campos – SP – 12228-970

Abstract. *The laser treatment of WC-Co surfaces is a non contact technique which transfers a large amount of energy on a region well limited by the laser focus diameter. The absorption processes occur on the cemented carbide surface and, therefore, its reflectivity performs an important role in the efficiency of the laser treatment. The locally absorbed energy leads to a localized increase of temperature which may be followed by phase transformations (solid-state, melting or vaporization). The occurency of these transformations depends on the laser parameters (fluence, wavelength and temporal features), thermal properties and also on the condition of the WC-Co target surface. When a cemented carbide surface is irradiated by a pulsed laser beam, thermal stresses are developed during the heating and cooling cycle due to the rapid expansion/contraction cycle of the irradiated region. Depending on the material properties and on the laser pulse energy and duration, level of stresses above the elasticity limit can be generated. These stresses may result in plastic deformations and crack generation on the laser beam irradiated region. This is particularly true for the cemented carbides, due to their high melting temperatures and low heat conductivity, which cause high temperature gradients. High residual stresses occur due to the difference between the thermal expansion coefficients of the binder and carbides. Due to the thermal deformations, crack occurrence becomes possible. The melted cobalt flow towards the free surface may cause the superficial increase of cobalt concentration. A Nd:YAG frequency-doubled laser, diode-pumped by was used to texture cemented carbide substrates. This laser works in pulsed regime with repetition rates varying between 5 and 25 kHz. To evaluate how the beam power and the number of texturing passes cause changes on the cemented carbide surface, samples of carbide material were textured with fixed frequency of 10 kHz. The number of texturing passes varied from 1 to 5. The average beam power on the sample surfaces were 3, 6, 9, 12 and 15 W. An additional sample was submerged in a 4 mm layer of water during texturing, with the number of texturizing passes varying from 1 to 5 and average laser power on the surface of 15 W. The increase of laser power from 3 to 15 W increased the surface roughness. When simultaneously the number of texturing passes and the average power of the laser beam were varied, surface roughness did not vary significantly for lower laser power values. Moreover, the highest laser power created a certain periodicity in the textured cemented carbide surface which can be related to the distance between the texturing pulses. The cemented carbide surface microstructure is affected by the laser power and by the number of texturing passes. The crack formation on the textured surfaces depends on the number of texturing passes and on the laser intensity. Apparently there is an accumulated fluence energy threshold on the surface which leads to crack generation. The roughness values of the surfaces textured on air were higher than those made in the water.*

Keywords*: cemented carbide, laser texturing, surface roughness*

1. INTRODUCTION

The laser treatment of WC-Co surfaces is a non contact technique which transfers a great amount of energy on a well limited region by the laser focus diameter. The absorption processes occur on the cemented carbide surface and, therefore, its reflectivity performs an important role in the efficiency of the laser treatment. The locally absorbed energy leads to a localized increase of temperature which may be followed by phase transformation (fusion, vaporization). The efficiency of these transformations depend on the laser parameters (fluence, wave length, temporal features), thermal properties and also on the condition of the WC-Co target surface (Dumitru et al., 2005).

When a cemented carbide surface is irradiated by a pulsed laser beam, thermal stresses are developed during the heating and cooling cycle due to the rapid expansion of the irradiated region. Depending on the cemented carbide material properties and on the laser pulse energy and duration, level of stresses above the elasticity limit can be generated. These stresses may result in plastic deformations and crack generation on the laser beam irradiated area. This is particularly true for the cemented carbides, due to their high melting temperatures and low heat conductivity, which cause high temperature gradients. High residual stresses occur due to the difference between the thermal expansion coefficients of the binder and carbides. It can be shown, using numerical simulation, that the temperature gradient in the titanium and tantalum carbides which may be present in the cemented carbide composition is higher than in tungsten carbide close to the surface. Due to the thermal deformations, crack occurrence becomes possible. The melted cobalt flows toward the free surface may cause the superficial increase of cobalt concentration (Yilbas et al., 2007).

1.1. The influence of the laser parameters on the results of laser treatment

A suitable combination of laser fluence and number of pulses must be applied on a cemented carbide surface to selectively remove cobalt from the surface with the ablation caused by the pulsed laser. The fluence of an ultraviolet laser (λ = 308 nm τ_p = 30 ns) must be higher than 1 J/cm^2 and lower than 4 J/cm^2 to selectively remove cobalt from the cemented carbide surface. Under high fluence, the cemented carbide presents an irregular fusion pattern, having a lot of holes for the escape of gases with average sizes of 3 to 5 μm scattered on the surface. These holes are probably generated by the escaped of gases which were generated in a violent ablation process which also transported tungsten and cobalt (Li et al., 2001b). Either beams of excimer laser or industrial lasers with fluence around 2.5 J/cm^2 are suitable to promote the selective removal of cobalt or, therefore, to generate the increase of diamond coating film adhesion applied after the laser treatment on the surface (Dumitru et al., 2005).

Comparing samples irradiated with CO_2 pulsed laser (λ = 10,6 μm and τp = 80ns) with samples irradiated with ArF laser (λ = 193 nm and τp = 30 ns), apparently the CO_2 laser is more effective for the cobalt removal, generating also higher damage to the substrate due to the higher fluence used compared with ArF laser (Cappelli et al., 1999).

Holes on a cemented carbide surface can be made using a saphire laser pulsing at 1 kHz in a focus diameter of 25 μm with fluence of 2, 5 and 10 J/cm^2. High fluence values like 10 J/cm^2 of this short pulse laser (τp = 100 fs) corresponds to a power density value little lower than 10^{14} W/cm^2, higher than the necessary limit to form an explosive plasma in the air (~ 10^{13} W/cm^2). In these cases, the plasma formation close to the focal plane scatters the laser beam, what reduces the fluence in the center of the beam and the ablation efficiency, generating instabilities in the drilling process and in the accuracy of the hole shape (Dumitru et al., 2004). Metallographic analysis of the hole walls made with this laser did not show any metallurgical change when the fluence was 2 and 5 J/cm^2 (Dumitru et al., 2003).

For the machining of different shapes and microgeometries with peaks and valleys, values between 10 and 20 J/cm^2 (with associated power of 0.5–1 x 10^9 W/cm^2) lead to good results. The machining of cemented carbide with *fs* pulse time length with fluence of 2 J/cm^2 leads to a complete lack of heat affected zone. It is important to observe that the energy density can be adjusted through the choice of optical parameters integrated with filters, beam expanders, focusing objectives (Dumitru et al., 2005).

The material processing with laser is governed by physics of the laser interaction with the material. The laser energy interacts first with the free electrons. The portion of the energy which is absorbed by the material propagates through the electron layers and is transferred to the crystalline structure. The material treatment thermal phenomenon is governade by relationship between the electron cooling time (around 1 ps), crystalline structure heating time and time duration of the laser pulse. In the processes where the laser time duration is of milliseconds order or even infinite (continuous lasers) the heat transfer classical laws are completely suitable to model the phenomenon. Fusion occurs and the material is thermally affected. Laser cutting applied of materials is an example of this case. When the pulse duration is of nanoseconds order, the main mechanism of energy loss is through conduction inside the solid. As a result of the laser interaction, the material first melt and, when the beam is powerful enough, evaporation occurs. The heat affected zone in this process is much smaller than in the previous situation. Laser drilling and engraving are typical processes in this time scale in which a small fusion is followed by a rapid evaporation. In switched lasers with pulse duration of nanoseconds order, the main mechanism of material removal is ablation, but a substantial fusion will be present when the interaction occurs with metallic materials (Yao et al., 2005).

In the interaction with cemented carbide, for the laser pulse of nanoseconds, the energy transfer occurs in thermal equilibrium during the pulse. The material removal happens basically through fusion and vaporization and, in these cases, the thermal properties of the carbide and cobalt grains play an important role. These materials have close heat conductivity (WC: 60–80 W/m K, Co: 70–75 W/m K), but present different fusion behavior. The melting point of Co is 1495° C and its ebullition temperature, 2927° C, is close to the WC melting point (2870° C). The partial fusion of Co starts between 1250 and 1300° C due to a eutectic reaction. The melting point of the eutectic binary is 1310° C, while the eutectic temperature of the ternary compound W-C-Co is 1280° C. Further increases in temperature causes additional dissolution of WC and complete melting of Co. At the same time, the smallest WC grains dissolve in the liquid and precipitate again, creating new larger WC grains. According to the WC-Co properties, the Co phase melts, vaporize and the material ablation occurs mainly by the selective removal of the binder. Therefore the WC grains can be removed by either, the ejection of melted Co or by the CO vapor. For high energy density, temperatures higher than the melting point may be reached and, in these situations, larger grains can show up due to the WC fusion (Dumitru et al., 2005).

For a laser with wave length of 308 nm, with pulse duration of 20 ns and working at repetion rate of 1 kHz, the limit to the ablation of pure Co is 0.6 J/cm^2 and the ablation rate increases linearly up to the fluence of 3 J/cm^2. The rate decreases smoothly up to the fluence of 9 J/cm^2. For higher fluencies, the vapor resulting from ablation absorbs the energy of the emitted laser, reducing the increase of the ablation rate on the surface. Further increase on fluence generates ionization growth of vapor particles, inducing plasma formation. This plasma leads to the creation of a "shield" which separates the surface from the input energy and, consequently, saturates the ablation rate. Due to the

attenuation of the input laser by the expanding plume generated by ablation, the ablation rate is higher for small beam diameters directed towards the surface (Li et al., 2001e).

The increase of the number of laser passes generates loss of carbon in the carbide grains affected by the laser. The original WC grains are transformed in non estequiometric phases of carbides like β-WC_{1-x}, α-W_2C, CW_3 and finally W (Li et al, 2001a). Therefore it is obvious that there is a loss of carbon during the cumulative processes of ablation causing the formation of a non estequiometric carbide and tungsten. This effect could be credited first to the successive fusions of WC grains caused by the pulsed irradiation which makes easier the reaction of the carbon in the tungsten carbide with oxygen of the air to form volatile gases like CO or CO_2 (Li et al, 2001d). Using X-ray diffraction test carried out on a textured surface with 32 passes, with power density of 137 MW/cm^2, Arroyo (2009) proved the presence of β-WC_{1-x} phase, which indicates structural changes and loss of carbon. As the power density increased from 137 MW/cm^2 to 239, 273, 308 and 410 MW/cm^2, new phases of α-W_2C, CW_3 poorer in carbon, showed up on the cemented carbide surface.

1.2. The use of water in the laser processing

The use of water in the material laser processing aims to make feasible the conversion of part of the light energy for vaporization and for the formation of plasma with mechanical impulse. The formation of shock waves in the liquid transports fragments and particles from the surface. The water also cools the surface more effectively than gases and, in some cases, the water and the products of its dissolution chemically reacts with the material.

The advantages and disadvantages of the use of water are summarized in table 1.

Table 1. Advantages and disadvantages of the material laser processing assisted by water (Kruusing, 2004).

Advantages	Disadvantages
Light transportation is possible along the water jet	Light is absorbed by water (what may be useful) and by fragments produced during processing
High pressure plasma due to confinement	Light may be scattered on the water surface, suspended elements and bubble generation
The water convection/explosive evaporation transport the fragments generated	Loss of power due to water cooling
More effective cooling of workpiece and ejected material	Harmful chemical reactions with water
Utility of chemical reactions with water	Water photolysis – Danger of explosion
Reduction of air environment pollution by gases and aerosols	Slow processing due to the long time of relaxation of water in vaporized state
High level of optical breakdown compared with air	More sophisticated equipment
Small focal point	Water and vapor are harmful to the electronic

Many of these effects can be obtained with other neutral liquids, but the water is the most common, cheap and safe. The water also has a high thermal capacity. The majority of research works made on this subject was carried out with pulse time of 10 – 100 ns using either excimer laser or laser Nd:YAG. There is a tendency of using shorter and shorter pulses in order to obtain better results, what in many cases demands a low energy density of the laser beam to have the same effect (Kruusing, 2004).

In most cases, in the material processing with water assisted laser (cutting, cleaning, mechanical shock processing), it is better that the water does not absorb light. Due to the absorption, the light intensity decreases as it propagates inside the water. The absorption length is higher than 10 m for wave length between 511 and 532 nm, a little higher than 10 mm for wavelength of 1054 to 1064 nm and just 1 μm for wavelength of 2940 nm measured in pure water at 298 K.

2. EXPERIMENTAL PROCEDURE

2.1. The laser source

A Nd:YAG laser system, doubled in frequency and pumped by diodes was used to texture the tools used in this work. This laser works in pulsed regime, with variable repetition rate between 5 kHz and 25 kHz. The operational features of the laser used are pointed out in table 2.

Table 2. Features of the laser source system

Wavelength	532 nm
Operation frequency	Fixed in 10 kHz
Pulse width	130 ns
Energy estability	< 0,08 % rms
Beam diameter	5 mm nominal
Maximum power	45 W

2.2. The texturing system and procedures

The reduction of the beam diameter from 5 mm of the laser source to a diameter of 0,1mm on the surface being textured occurs due to a set of lenses which directs the beam to a scanning galvanometric system (see figure 1). This system guarantees a precise position of the laser pulses on the sample surface. The use of this system causes a loss of light power, making the incident energy on the surface being textured 1/3 of the output laser source energy.

Thirty cemented carbide surfaces were textured. Twenty Five were textured in air with average power varying from 3 to 15 W in increments of 3 W and number of texturing passes varying from 1 to 5. Five surfaces were textured under a 4 mm layer of water, with an incident average power of 15 W and number of texturing passes varying from 1 to 5. Table 3 presents the properties of the laser pulse on the interaction region with cemented carbide. The constant parameters were the focus diameter of the laser beam on the surface (0.100 mm), the temporal width of the pulse (130 ns), the laser frequency (10 kHz) and the distance between the centers of the pulses (0.07mm).

Table 3. Properties of the incident laser pulse on the cemented carbide sample

Average power [W]	**3**	**6**	**9**	**12**	**15**
Peak power [kW]	2.31	4.62	6.92	9.23	11.5
Pulse energy [mJ]	0.3	0.6	0.9	1.2	1.5
Irradiance [MW/cm^2]	29.4	58.8	88.1	118	147
Fluence [J/cm^2]	3.82	7.64	11.46	15.28	19.1
Focus diameter	0.1 mm				

In the experiments where it was necessary to increase the number of texturing passes, the scanning direction was tilted in such a way that, when the surface received a second texturing pass, a rotation angle was applied. For all the other texturing where *n* passes were applied on the surface, an incremental rotation of 180/n degrees was applied.

When the texturing was over, the samples were qualitatively analyzed in optical microscope. Besides that, they had their surface roughness measured. After that, all the samples were analyzed in a scanning electronic microscope.

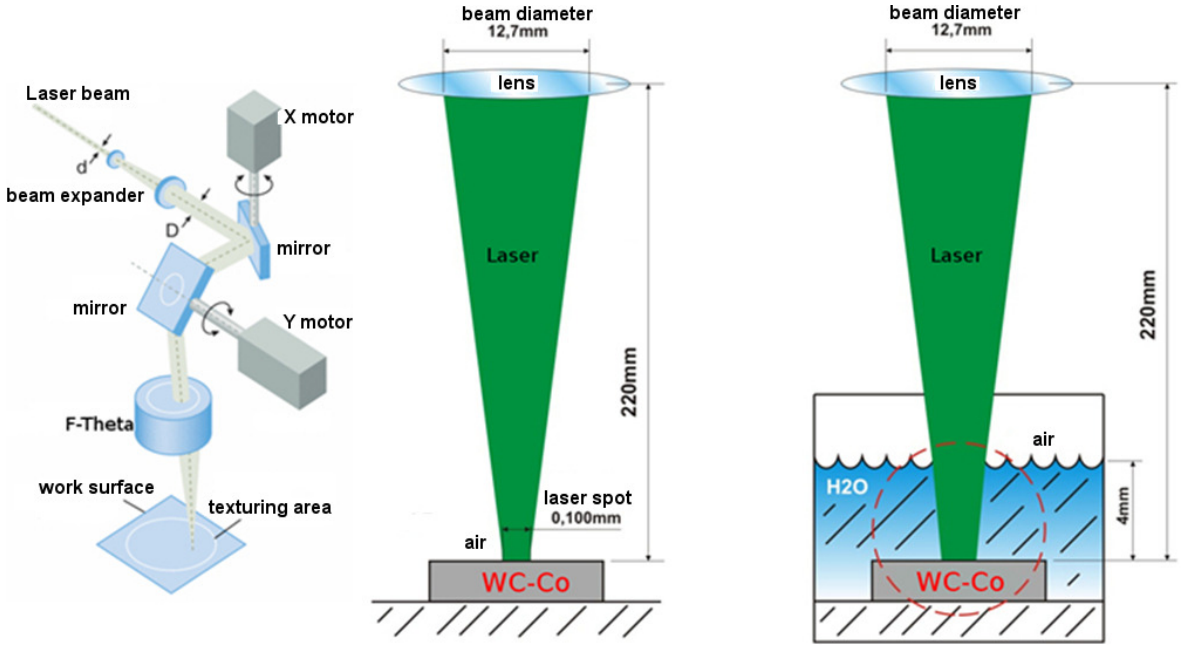

Figure 1. Scheme of the laser texturing system

3. ANALYSIS OF THE RESULTS

Laser texturing is the scanning of a surface with laser pulses of short duration. The distance between the pulses is such that all the surface interacts with the laser due to the pulse superposition (figure 2a). Each pulse, in its interaction with the surface can, depending on its power, causes fusion and ablation of the material and to promote surface micro alterations.

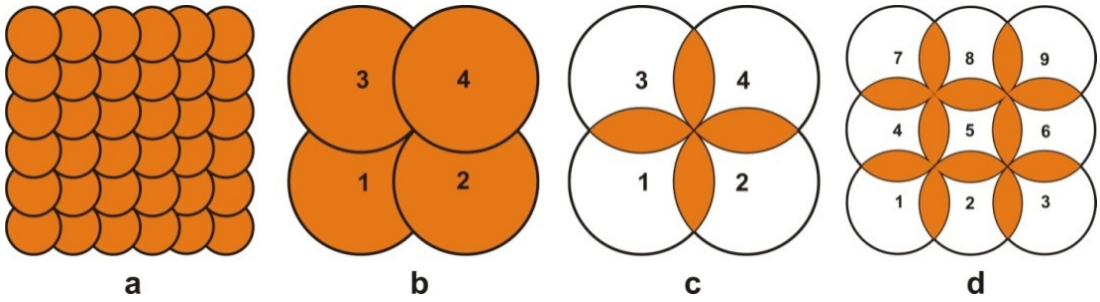

Figure 2. Geometrical aspects of texturing: (a) superposition of texturing pulses, (b) sequencing of pulses (c) super exposed areas, (d) formation of texturing patterns.

The pulse superposition generates areas which will be exposed more than once to the laser interaction. Figure 2b shows the minimum superposition necessary of four pulses to guarantee a total coating of the surface. The resulting areas of intersection can be seen in figure 2c. The central regions of the pulses are numerically indicated in the sequence they reach the surface being textured. The exposition of the surface to the laser beam generates heat and fusion, evaporation and ablation may occur, depending on the time and energy of the pulse. The regions shown on figure 2c identify areas exposed twice to the laser due to pulse superposition. A pattern of surface exposition like the one indicated in figure 2d could be generated when a set of nine sequential pulses with 30% degree of superposition is used. In this figure, due to the interaction with the pulses, the central region of the pulse 5 is surrounded by four arcs belonging to the neighbor pulses and identify a textured area with just one interaction. The regions of pulse intersections received two interactions. These regions could be the location of depressions formed on the surface due to the doubled exposition of the material to the laser beam.

3.1. Roughness of the surfaces textured in air

The roughness of the cemented carbide surfaces were measured both, before and after the laser interaction. Table 4 shows the values obtained in these measurements.

Table 4. Laser effect on the roughness of the surfaces - *Ra* [μm].

Power [W]	Number of texturing passes (N)				
	1	2	3	4	5
3	0.33	0.33	0.34	0.33	0.33
6	0.51	0.51	0.51	0.50	0.50
9	0.42	0.43	0.43	0.43	0.43
12	0.59	0.61	0.57	0.59	0.59
15	0.59	0.5	0.62	0.47	0.67
Without texturing	0.26 +- 0.023				

In the last row of this table it is registered the average roughness and the standard deviation of a total of 25 measurements carried out in 5 cemented carbide samples before the laser treatment. The graphical representation of table 4 data (figure 3) shows that the roughness of the textured surfaces are always higher than the surface roughness without texturing. Roughness is not significantly influenced by the number of texturing passes up to the power of 12 W. A possible explanation can be the adopted texturing strategy which kept constant the superposition factor of the pulses.

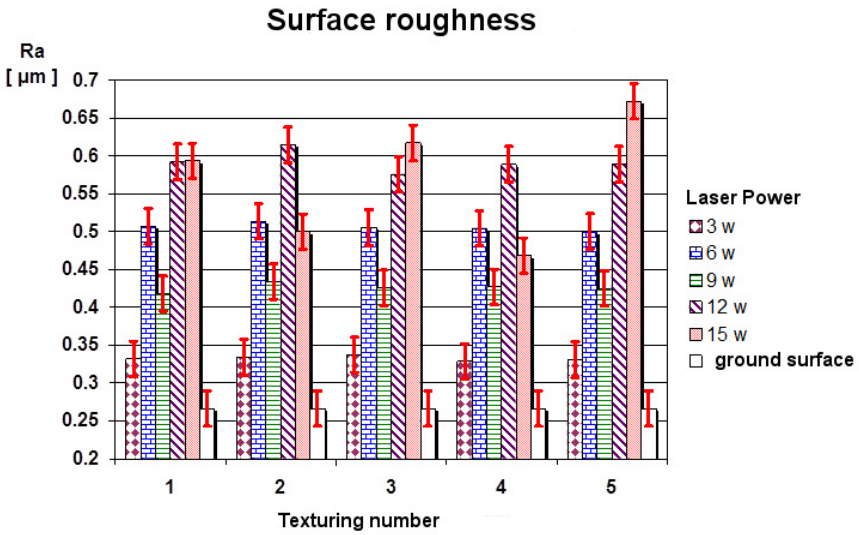

Figure 3. Roughness of the textured cemented carbide surfaces

Another factor which may have contributed to the low variability of surface roughness as the number of textruing passes increased was the rotation between the texturing planes of from one pass to the next. The surface roughness grew as the laser power increased, except for the experiment with 9w.

The Abbott-Firestone curve is built starting in the highest peak of the roughness profile towards the lowest valley, measuring progressively the cumulative fraction of the profile (Torrance. 1997). It is basically a representation of the amount of material related to the cutting level of the roughness profile. Its projection allows the identification of the parameters *Mr1*. *Mr2*. *Rk*. *Rpk* e *Rvk*.

The comparison of different Abbott–Firestone curves can be complex due to the large dispersion of roughness heights which can occurr according to the surface being measured (Buj Corral et al., 2010).

In the surfaces textured with the lowest power, 3 W, the *Rk* parameter measured in the texturing passes from 1 to 5 presented an average value of 1.08 µm with variation of roughly 6 %.

The roughness values of the textured surfaces with 15 W with number of texturing passes of 1, 2, 3, 4 and 5 were respectively 0.59 µm, 0.50 µm, 0.62 µm, 0.47 µm and 0.67 µm *Ra* (table 4) and the *Rk* values were respectively 1.51 µm, 1.52 µm, 2.04 µm, 1.5 µm and 2.05 µm. The *Ra* parameter presented high values in the surfaces textured 1, 3 and 5 times and the lower values in the surfaces textured 2 and 4 times. The *Rk* value reflects the surface roughness and, therefore, the *Rk* of the surface which was submitted to just one pass of texturing should be higher. In figure 4 the Abbott-Firestone curves for the surfaces submitted to 1 and 3 texturing passes can be seen. It can be noticed in this figure a difference of 26% in the *Rk* values of these 2 surfaces through the difference of the slopes of the linear portions of the curves. It can also be seen that these two surfaces presented difference in the *Mr1* values.

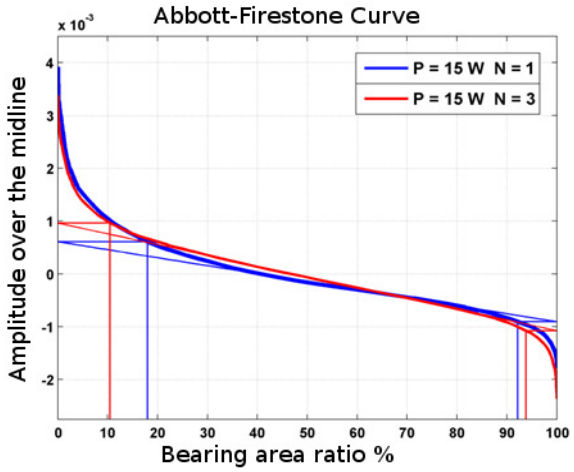

Figure 4. Abbott-Firestone curves of the surfaces with one and three texturing passes

The surface submitted to just one texturing pass presented *Mr1* of roughly18%, while the surface submitted to 3 textruing passes presented *Mr1* close to 10.5%. The higher value of *Mr1* means that the surface textured just once with power of 15 W has a *Ra* value high compared with the other surfaces textured with the same power and *Rk* low when compared with the other surfaces textured with the same power. The existence of a higher frequency of peaks *Rpk* summed to the low value of *Rk* justifies the high *Ra* value in the surface submitted to just one texturing pass. The texturing carried out with power of 3 W did not significantly influenced the *Mr1* parameter when compared with the non textured surfaces. Surfaces textured with 3 W and without texturing presented the same average *Mr1 value of* ~ 8%. From the texturing power of 6 W on, the *Mr1* parameter increased from 8 % to 12 %. Its average value was 10 % for power texturing of 9 W and 11.5 % for texturing with 12 w. Just or the surface submitted to one texturing pass with power of 15 W this value increased steeply to 18% as already mentioned.

The *Rpk* and *Rvk* values of the non textured surfaces were low and tend to increase with the number of texturing passes. In the non textured surfaces *Rpk* values was lower than *Rvk*. In the texturing with 3 W de *Rpk* e *Rvk* increased, but *Rpk* increased more than *Rvk*, what means that texturing increased the surface roughness, increasing much more the height of the peaks than the depth of the valleys. As the texturing carried out with 3 W did not increased the *Mr1* value, it could be concluded that the increase in the *Ra* values of the textured surfaces was caused by the increase of the amplitude of the surface peaks. For higher power *Rpk*/Rvk ratio overcame 1.5, reaching na average value of 1.9. The exception was the surface textured with 15 w.

Using *Ra* parameter evaluation is not possible to differentiate the surfaces submitted to several texturing passes from those submitted to just one texturing pass, regardless the laser power used, as shown in figure 3. The frequency distributions of the surface roughness without texturing and textured with low power were close to normal distribution. Figure 5a shows this fact for the surface textured with just one texturing pass and power of 3 w. The same is valid for power 6. 9 and 12 w, regardless the number of texturing passes. When the surface was textured with one pass and 15 W of power, the frequency distribution is far from normality. The existence of signals at the right of the normal curve is related to higher values of *Rpk* and *Mr1* and the lack of signals at the left of the curve is related to the low values of *Rvk* and low values of (100 – *Mr2*). The existence of high frequency signals close to the average in the left side of the normal curve indicates the existence of a high quantity of shallow valleys which makes *Rk* value.

The application of Fourier transform in the roughness function of the cemented carbide surface textured with low power always presented curves similar to those obtained in non textured surfaces. No periodicity was found for the texturing power from 3 to 12 W, regardless the number of texturing passes. For the highest power a peak related to the periodicity of 14.16 mm^{-1} was always present (figure 5b).

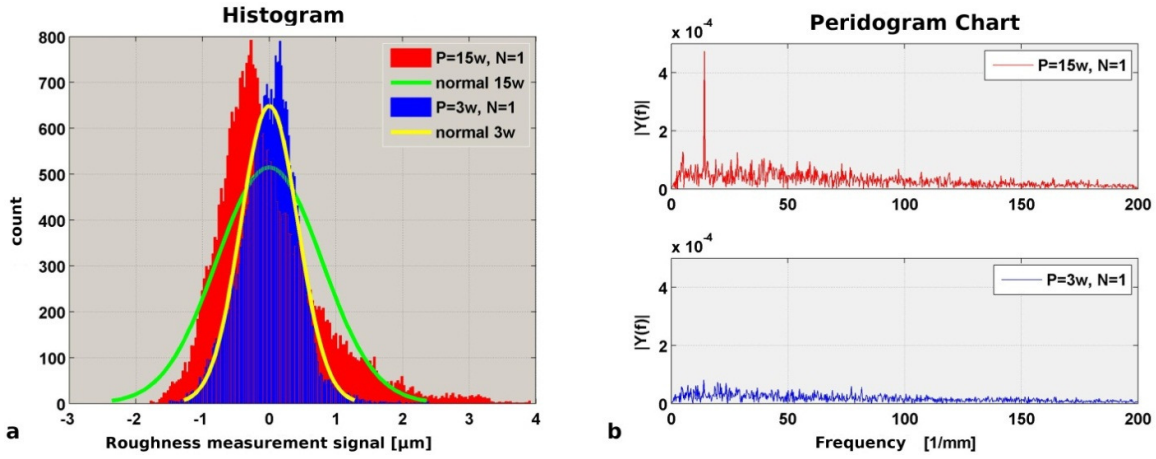

Figure 5. Alterations in the roughness data distribution versus texturing power .

It means that in a 1 mm interval is occurring 14.16 periodical repetitions of a property associated to the texturing which is influencing the roughness function. The distance between each one of these signals present in the roughness function and which present a repetition pattern detected by the Fourier transform is 0.07 mm. The texturing parameter which can be related to the wavelength of 0.07 mm is the distance between successive pulses. This parameter, kept constant in all experiments, was just safely identified in the roughness of the surfaces textured with 15 W power. Therefore, it can be concluded that just in this condition ablation was severe enough to leave marks on the surface. The intensity of the peak of periodicity is related to the signal amplitude. As the number of texturing passes varied, the intensity of the signal also varied. With two texturing passes the peak intensity was reduced from 4.8 to 2. This fact can be explained by the rotational imposed between the two texturing pass and displacement between the center of rotation

and the center of the texturing laser system, which generates conditions for a destructive interference. However, with 15 W power, no matter the number of passes, the typical ondulation related to the texturing process was detected in the roughness function (see figure 5b). The interaction between laser and cemented carbide surface is strongly influenced by the average power of the incident beam.

Summarizing, it can be stated that the laser texturing of the cemented carbide increases the *Ra* surface roughness parameter. This increase with the growth of texturing power is caused by the increase in the *Rk* value, which also grows with the laser power. The laser power also increases *the Mr1* value. Moreover, the *Rpk/Rvk* ratio, which in the non textured surface was 0.6, was close to 2 in the textured surfaces.

3.2 The fluence effect and the crack generation.

The five levels of incident power combined with the number of texturing passes carried out on the surfaces allow to identify each one of the surfaces by the amount of energy accumulated per unit of area (fluence). The texturing process consisted of the application of successive pulses up to the point the surface was totally textured. Therefore, a new energy input in a same region just would happen after the end of a phase of the process. Table 5 shows the fluence values calculated for each one of the twenty five textured surfaces.

Table 5. Accumulated Fluence [J/cm^2]

	Number of texturing passes (N)				
Power [W]	1	2	3	4	5
3	3.82	7.64	11.46	15.28	19.10
6	7.64	15.28	22.92	30.56	38.20
9	11.46	22.92	34.38	45.84	57.30
12	15.28	30.56	45.84	61.12	76.39
15	19.10	38.20	57.30	76.39	95.49

The metalographic analysis of the surfaces submitted to the same fluence can be seen in figure 6. It can be seen in this figure that the higher the incident laser power the higher was the severity of laser interaction with cemented carbide. The final roughness was lower for the surface textured with the lower power and higher number of passes. The textured surface with power of 3 W and 4 texturing passes (figure 6a) presented roughness *Ra* = 0.33 µm, while the surface textured with 6 W and 2 passes had *Ra* = 0.51 µm (figure 6b) and, finally, the surface textured with 12 W and just one pass presented *Ra* = 0.59 µm (figure 6c). In all these surfaces, the accumulated fluence was 15.28 J/cm^2. The microstructures were thinner in the textured surfaces with the lower power of the laser beam.

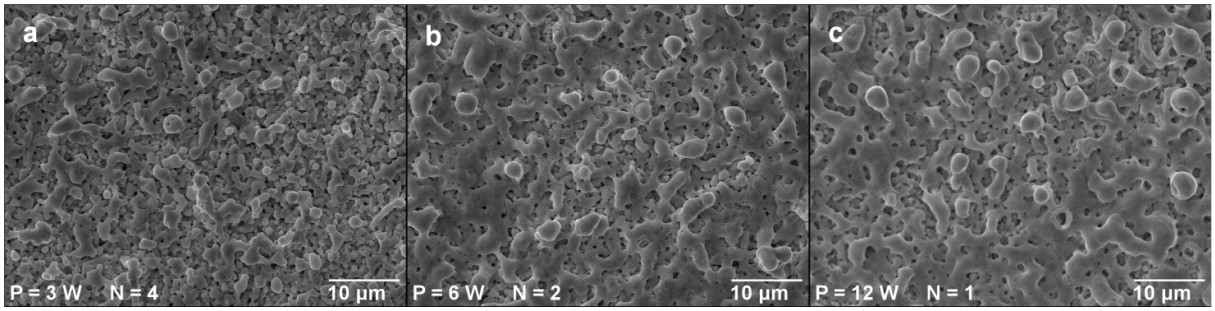

Figure 6. Textured surfaces with the same accumulated fluence - 15.28 J/cm^2.

Among the 25 textured surfaces, 13 presented cracks which could be observed in the electronic microscope and are grouped in the table 5 in grey tone. Apparently cracks show up in a range of fluence between 22.92 and 30.56 J/cm2. The surfaces submitted to an accumulated fluence higher than 22.92 J/cm2 presented a texture which indicates fusion of almost all the irradiated surface. Very likely, the cracks were caused by the fast cooling of the melted material, which generates tensile stresses higher than the material could support. As the accumulated fluence grew, the presence of cracks was more pronounced, increasing the fragility of the melted layer.

3.3 The influence of the water layer in the microstructure and roughness of the textured surfaces

Figure 7 shows the microstructures of the surfaces submitted to texturing in air and under a water layer of 4 mm. Figure 7a shows a surface treated with 15 W and 3 texturing passes and figure 7b shows a surface textured in water under the same conditions. The surface of figure 7a (accumulated fluence of 57.30 J/cm^2) was totally melted under the laser beam, with cracks typical of the cooling of melted material. In the figure 7b (the only difference from figure 7a is the water layer used in the laser treatment) the structure is made of fine grains, very different from the surface textured in air. As the thickness of the liquid covering the surface was just 4 mm and the laser wavelength was 532 nm, it can be inferred that there was not attenuation of the incident energy on the samples under water, since the absorption length Δ is higher than 10 m for the laser wavelength used in the experiments.

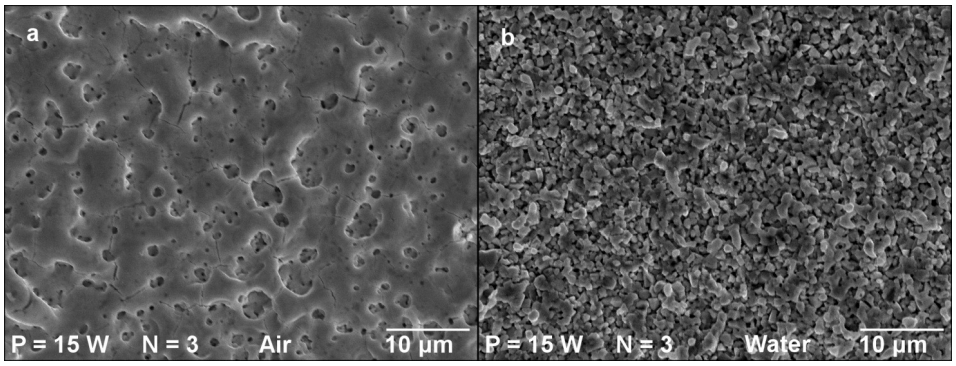

Figure 7. Pictures of the surfaces textures with and without the presenece of water

When the laser pulses reach the water, it is not attenuated due to the laser wavelength and the small thickness of the water layer. The laser beam is submitted to refraction and, therefore, the focus diameter on the textured surface is higher, reducing, consequently the fluence and the power density. Even in this condition, the incident beam was able to increase the surface temperature generating fusion and ablation. The order of magnitude of the power density typical of the "shoot peening" laser processing is around 1-100 GW/cm^2 (Kruusing. 2004) and the values reached in this work were two orders of magnitude lower. The values of power density were also smaller than those used in "microscale laser shock peening" treatment (Chen et al., 2004). Therefore, it is not expected that the plasma collapse generated by the restricted ablation could induce in the liquid shock waves able to generate high compressive residual stresses in the material. Very likely, after the end of the plasma expansion, the shock between the liquid and the melted cemented carbide avoided the formation of a coarse structure due to the high cooling speed of the water compared with the air. Moreover, the shock between the melted metal and the water increased the cleaning effect. This interaction mechanism between laser and cemented carbide in the interface cemented carbide-liquid probably explain the different textures obtained in air and under water. Figure 8 shows a comparison between the roughness of the surfaces textured under water and in air.

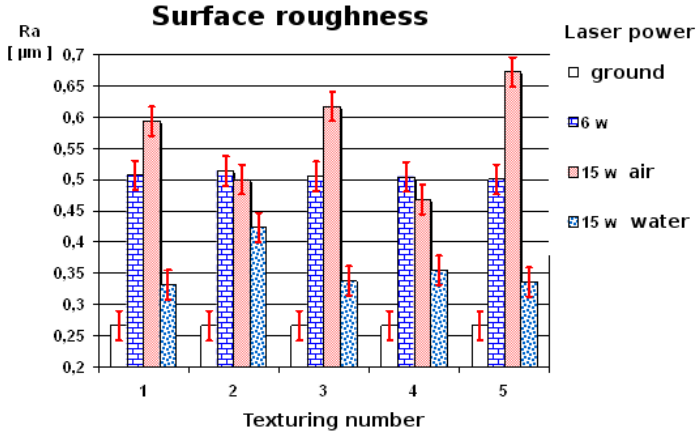

Figure 8. Influence of the use of water in the roughness of the textured surfaces

The low roughness values of the surfaces treated under water compared with those treated in the air confirms the refined structure shown in the metallographic analysis.

4 CONCLUSIONS

The texturing of cemented carbide surfaces with Nd:YAG laser,operating at 10 kHz with average power ranging from 3 W to 15 W, generates roughness that increase with the laser power texturing.

The roughness surface does not suffer interference from the texturing number of lower average laser power.

The higher texturing power generates on cemented carbide surface periodicity which may be related to the distance between centers of successive texturing laser pulses.

The surface microstructure is affected by the texturing laser power and the texturing number. Higher laser power texturing affect the surface structure much more than texturing number. Small surface structural changes are obtained with lower laser texturing power.

The presence of cracks on textured surfaces depends on average texturing power and the texturing number. Apparently there is a threshold of accumulated fluence on the surface that leads to the generation of cracks by texturing.

The environment texturing in air generates higher roughness in the cemented carbide substrate surface than underwater laser texturing.

5. REFERENCES

Arroyo, Jose Manoel. Investigação sobre o Uso da Texturização a Laser na Preparação da Superfície a Ser Recoberta em Ferramentas de Metal Duro para Fresamento. Tese de Doutorado. Universidade Estadual de Campinas. Campinas. 2009.

Buj Corral, I., Calvet, J.V., Salcedo, M.C., 2010. Use of roughness probability parameters to quantify the material removed in plateau-honing. International Journal of Machine Tools & Manufacture. n.50. p.621–629.

Cappelli, E., et al., 1999. WC–Co cutting tool surface modifications induced by pulsed laser treatment. Applied Surface Science. v.138-139. n.1-4. p.376-382.

Chen, H., Kysar, J.W., Yao, Y.L., 2004. Characterization of Plastic Deformation Induced by Microscale Laser Shock Peening. Journal of Applied Mechanics. v.71. p.713-723.

Dumitru, G., et al., 2003. Metallographical analysis of steel and hard metal substrates after deep-drilling with femtosecond laser pulses. Applied Surface Science. v.208-209. n.1. p.181-188.

Dumitru, G., et al., 2004. Femtosecond laser ablation of cemented carbides: properties and tribological applications. Applied Physics A: Materials Science and Processing. v.79. n.3. p.629-632.

Dumitru. G., et al., 2005. Laser processing of hardmetals: Physical basics and applications. International Journal of Refractory Metals and Hard Materials. v.23. n.4-6. p.278–286.

Kruusing, A., 2004. Underwater and water-assisted laser processing: Part 1 - General features. steam cleaning and shock processing. Optics and Lasers in Engineering. v.41. n.2. p.307-327.

Li, T., et al., 2001a. Phase transformation during surface ablation of cobalt-cemented tungsten carbide with pulsed UV laser. Applied Physics A: Materials Science and Processing. v.73. n.3. p.391-397.

Li. T., et al., 2001b. Selective removal of cobalt binder in surface ablation of tungsten carbide hardmetal with pulsed UV laser. Surface And Coatings Technology. v.145. p.16-23.

Li. T., et al., 2001d. Escape of carbon element in surface ablation of cobalt cemented tungsten carbide with pulsed UV laser. Applied Surface Science. v.172 p.51-60.

Li, T., et al., 2001e. Ablation of cobalt with pulsed UV laser radiation. Applied Surface Science. v.172. p.356-365.

Torrance, A.A., 1997. A simple datum for measurement of the Abbott curve of a profile and its first derivative. Tribology International. v.30. n.3. p.239-244.

Yao, Y.L., Chen, H., Zhang, W., 2005. Time scale effects in laser material removal: a review. International Journal of Advanced Manufacturing Technology. v.26. n.5-6. p.598-608.

Yilbas, B.S., et al., 2007. Cemented carbide cutting tool: Laser processing and thermal stress analysis. Applied Surface Science. v.253. p.5544-5552.

6. RESPONSIBILITY NOTICE

The authors are the only responsible for the printed material included in this paper.